

# Engineered Nanoforce Gradients for Inhibition of Settlement (Attachment) of Swimming Algal Spores

James F. Schumacher,<sup>†</sup> Christopher J. Long,<sup>‡</sup> Maureen E. Callow,<sup>§</sup> John A. Finlay,<sup>§</sup>  
James A. Callow,<sup>§</sup> and Anthony B. Brennan<sup>\*,†,‡</sup>

*J. Crayton Pruitt Family Department of Biomedical Engineering and Department of Materials Science and Engineering, University of Florida, Gainesville, Florida 32611-6400, and School of Biosciences, University of Birmingham, Birmingham, United Kingdom*

Received November 2, 2007. In Final Form: December 19, 2007

Current antifouling strategies are focused on the development of environmentally friendly coatings that protect submerged surfaces from the accumulation of colonizing organisms (i.e., biofouling). One ecofriendly approach is the manipulation of the surface topography on nontoxic materials to deter settlement of the dispersal stages of fouling organisms. The identification of effective antifouling topographies typically occurs through trial-and-error rather than predictive models. We present a model and design methodology for the identification of nontoxic, antifouling surface topographies for use in the marine environment by the creation of engineered nanoforce gradients. The design and fabrication of these gradients incorporate discrete micrometer-sized features that are associated with the species-specific surface design technique of engineered topography and the concepts of mechanotransduction. The effectiveness of designed nanoforce gradients for antifouling applications was tested by evaluating the settlement behavior of zoospores of the alga *Ulva linza*. The surfaces with nanoforce gradients ranging from 125 to 374 nN all significantly reduced spore settlement relative to a smooth substrate, with the highest reduction, 53%, measured on the 374 nN gradient surface. These results confirm that the designed nanoforce gradients may be an effective tool and predictive model for the design of unique nontoxic, nonfouling surfaces for marine applications as well as biomedical surfaces in the physiological environment.

## I. Introduction

The biological response to a material placed within a natural aquatic or physiological environment is controlled by the surface characteristics of the material. This biological–surface interaction influences the biocompatibility of materials used in medicine<sup>1,2</sup> and the degree of biofouling on surfaces in the marine environment.<sup>3,4</sup> The field of biomaterials is typically associated with those materials used for medical devices and biomedical implants. For most synthetic biomaterials, the surface is designed to minimize the biological–surface interaction. Other biomaterials, like those used for tissue engineering and other specialized applications, are designed to facilitate the adhesion of preferred cells that promote the growth of replacement tissue and function. The study of marine biofouling focuses on the response of the settling (attaching) stages of organisms to man-made materials placed in the ocean. Ideal surfaces or coatings are antifouling [i.e., no settlement (attachment) of the colonizing larvae, spores, or cells] and/or fouling-release (i.e., organisms release under hydrodynamic forces because they are weakly adhered). With the recent environmental restrictions placed on antifouling paints,<sup>4</sup> non-biocidal coatings, biomaterials, and nontoxic surface modification techniques are being explored for marine applications. Subsequently, new and promising antifouling materials and

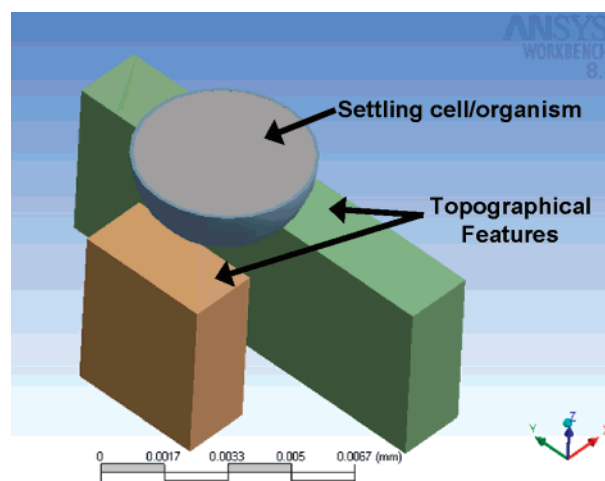


**Figure 1.** Schematic of a settling cell/organism contacting two dissimilar topographical features, effectively creating a stress gradient within the lateral plane of the membrane/body due to the difference in bending moments between the two geometrically dissimilar features and the strain on the membrane induced by the separation distance between the features.

designs that are developed may have applications as nonfouling surfaces in the biomedical field. Similarities exist between the early fouling events on the surface of a synthetic material in both the physiological and marine environments, including the formation of an organic conditioning film (e.g., proteins), bacterial adhesion, and biofilm formation.<sup>1–4</sup> However, in the more aggressive and varied marine environment, the microfouling community is more diverse and complex. It includes many types of algal cells while a climax marine community comprises a variety of macroalgae and invertebrates such as barnacles, tubeworms, and sponges.<sup>3,4</sup>

\* To whom correspondence should be addressed at the Department of Materials Science and Engineering, University of Florida, P.O. Box 116400, Gainesville, FL 32611-6400. Phone: (352) 392-6281. Fax: (352) 392-3771. E-mail: abrennan@mse.ufl.edu. Website: <http://brennan.mse.ufl.edu/>.

<sup>†</sup> J. Crayton Pruitt Family Department of Biomedical Engineering, University of Florida.

<sup>‡</sup> Department of Materials Science and Engineering, University of Florida.

<sup>§</sup> School of Biosciences, University of Birmingham.

(1) Castner, D. G.; Ratner, B. D. *Surf. Sci.* **2002**, *500*, 28–60.

(2) Tirrell, M.; Kokkoli, E.; Biesalski, M. *Surf. Sci.* **2002**, *500*, 61–83.

(3) Callow, M. E.; Callow, J. A. *Biologist* **2002**, *49*, 10–14.

(4) Yebra, D. M.; Søren, K.; Dam-Johansen, K. *Prog. Org. Coat.* **2004**, *50*, 75–104.

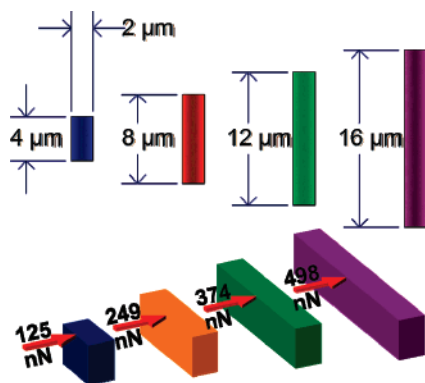


**Figure 2.** Estimated lateral forces required to cause a 10% end deflection of micrometer-sized topographical features in PDMS modeled as cantilever beams (3  $\mu\text{m}$  feature height).

Since the observations in the early 20th century on the effect of substrate structure on cellular behavior,<sup>5,6</sup> scientists and engineers have identified three main factors effective in controlling cellular response and function. These surface parameters include chemistry, topography, and mechanics and have been deemed as physicochemical cues.<sup>7</sup> A direct effect of surface topography and substrate mechanics is the mechanical forces exerted on and sensed by a settling and/or attaching cell. This phenomenon is known as mechanotransduction, and its characterization and manipulation have been studied in great detail for applications in cell and tissue engineering.<sup>8–10</sup> In the arena of marine biofouling, surface properties have been studied for applications such as antifouling and fouling-release coatings. Variations in surface chemistry, in relation to surface energy,<sup>11–13</sup> and surface topography to create superhydrophobic surfaces<sup>14,15</sup> have been used to control the settlement and adhesion of marine fouling organisms. However, most of these antifouling strategies do not consider the role of mechanotransduction in the design and modeling of nonfouling surfaces.

This paper presents a design methodology for the creation of nontoxic, antifouling surfaces for use in the marine environment based on mechanotransduction using nanoforce gradients. The design and fabrication of these gradients incorporate discrete micrometer-sized features that are associated with the species-specific surface design technique of engineered topography.<sup>16</sup> The effectiveness of nanoforce gradients for antifouling applications was tested by evaluating the settlement behavior of zoospores of the alga *Ulva linza*.

*Ulva* (syn. *Enteromorpha*) is a green macroalga that is common on seashores throughout the world and as a fouling organism on man-made structures, including ships. Dispersal and colonization of substrata is mainly through the production of vast numbers of motile spores (zoospores). Zoospores are pyriform, quadri-

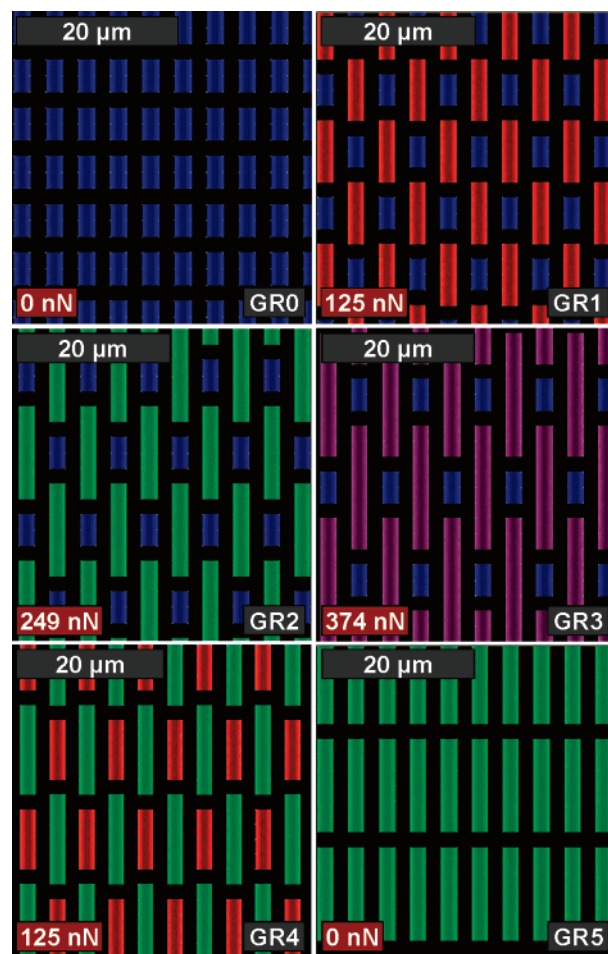


**Figure 3.** Pattern design of two-element engineered topographies representing a range of modeled nanoforce gradients. Feature colors correspond to feature length as identified in Figure 2. Gradient surface 1 (GR1), 4  $\mu\text{m}$  (blue) and 8  $\mu\text{m}$  (red) length features, and gradient surface 4 (GR4), 8  $\mu\text{m}$  and 12  $\mu\text{m}$  (green) length features, contained an estimated force gradient of 125 nN. Gradient surface 2 (GR2), 4  $\mu\text{m}$  and 12  $\mu\text{m}$  length features, included a force gradient of 249 nN. Gradient surface 3 (GR3), 4  $\mu\text{m}$  and 16  $\mu\text{m}$  (purple) length features, was designed at a force gradient of 374 nN. Gradient surface 0 (GR0), 4  $\mu\text{m}$  length feature, and gradient surface 5 (GR5), 12  $\mu\text{m}$  length feature, contained no force gradient, as neighboring features were the same.

flagellate cells, typically 7–10  $\mu\text{m}$  in length. The spore body is surrounded by a lipoprotein plasma membrane; there is no discrete cell wall in this dispersal stage. Once a swimming spore has located a suitable surface, it undergoes an irreversible commitment to settlement and adhesion, a process that involves the sequential loss of flagella, the exocytotic secretion of a preformed adhesive glycoprotein, and the production of a discrete cell wall.<sup>17</sup> Prior to permanent adhesion, the swimming spore undergoes characteristic presettlement behavior that involves a “searching” pattern of exploration close to the substratum.<sup>18,19</sup> A number of surface cues have been shown to moderate the way in which a spore interacts with the substratum, including wettability,<sup>20–22</sup> topography,<sup>16,23–25</sup> friction,<sup>26</sup> and microbial biofilms.<sup>27</sup> A role for rapid and transient changes in cytoplasmic calcium concen-

(5) Harrison, R. G. *Science* **1911**, *34*, 279–281.

(6) Harrison, R. G. *J. Exp. Zool.* **1914**, *17*, 521–544.

(7) Wong, J. Y.; Leach, J. B.; Brown, X. Q. *Surf. Sci.* **2004**, *570*, 119–133.

(8) Chen, C. S.; Tan, J.; Tien, J. *Annu. Rev. Biomed. Eng.* **2004**, *6*, 275–302.

(9) Dalby, M. J. *Med. Eng. Phys.* **2005**, *27*, 730–742.

(10) Reinhart-King, C. A.; Hammer, D. A. In *Principles of Cellular Engineering, Understanding the Biomolecular Interface*; King, M. R., Ed.; Academic Press: London, 2006; pp 3–24.

(11) Schmidt, D. L.; Brady, R. F., Jr.; Lam, K.; Schmidt, D. C.; Chaudhury, M. K. *Langmuir* **2004**, *20*, 2830–2836.

(12) Gudipati, C. S.; Finlay, J. A.; Callow, J. A.; Callow, M. E.; Wooley, K. L. *Langmuir* **2005**, *21*, 3044–3053.

(13) Yarbrough, J. C.; Rolland, J. P.; DeSimone, J. M.; Callow, M. E.; Finlay, J. A.; and Callow, J. A. *Macromolecules* **2006**, *39*, 2521–2528.

(14) Marmur, A. *Biofouling* **2006**, *22*, 107–115.

(15) Genzer, J.; Efimenko, K. *Biofouling* **2006**, *22*, 339–360.

(16) Schumacher, J. F.; Carman, M. L.; Estes, T. G.; Feinberg, A. W.; Wilson, L. H.; Callow, M. E.; Callow, J. A.; Finlay, J. A.; Brennan, A. B. *Biofouling* **2007**, *23*, 55–62.

(17) Callow, J. A.; Callow, M. E. In *Biological Adhesives*; Smith, A. M., Callow, J. A., Eds.; Springer-Verlag: Berlin, 2006; pp 63–78.

(18) Callow, M. E.; Callow, J. A.; Pickett-Heaps, J.; Wetherbee, R. J. *Phycol.* **1997**, *33*, 938–974.

(19) Heydt, M.; Rosenhahn, A.; Grunze, M.; Pettitt, M.; Callow, M. E.; Callow, J. A. *J. Adhesion* **2007**, *83*, 417–430.

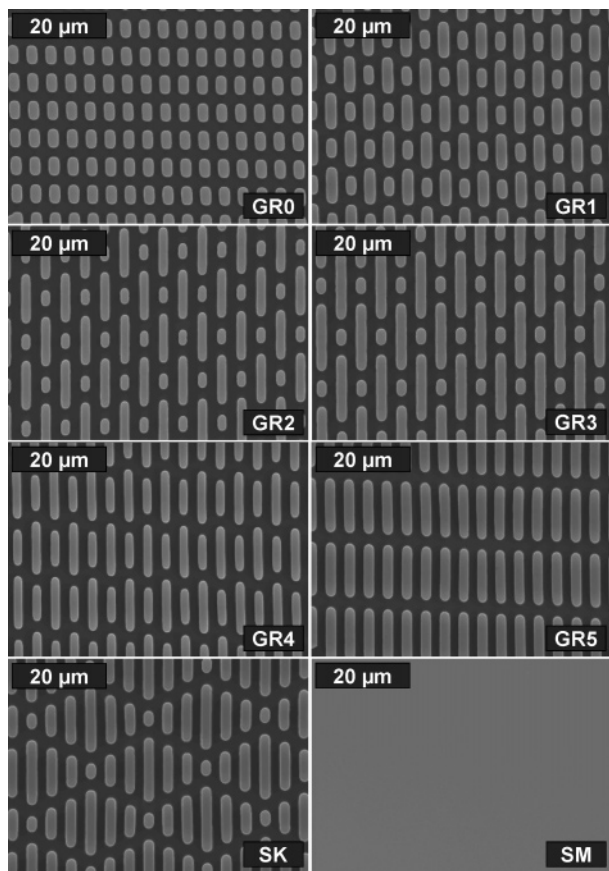


**Figure 4.** Scanning electron micrographs of force-gradient engineered topographies fabricated in PDMS<sub>e</sub> by replication of silicon wafer molds. GR0 and GR5 contain no force gradients; GR1 and GR4 contain estimated force gradients of 125 nN; GR2 contains a force gradient of 249 nN; GR3 contains a force gradient of 374 nN. The Sharklet AF (SK) engineered topography was included as a negative standard. A smooth PDMS<sub>e</sub> surface (SM) was included as a positive standard.

trations in settling spores has recently been detected.<sup>28</sup> This may form the basis of a calcium-based intracellular signaling pathway linking surface detection to the activation of adhesive secretion and associated cellular processes.

## II. Theory

We hypothesized that nanoforce gradients caused by variations in topographical feature geometry will induce stress gradients

(20) Callow, M. E.; Callow, J. A.; Ista, L. K.; Coleman, S. E.; Nolasco, A. C.; Lopez, G. P. *Appl. Environ. Microbiol.* **2000**, *66*, 3249–3254.

(21) Ista, L. K.; Callow, M. E.; Finlay, J. A.; Coleman, S. E.; Nolasco, A. C.; Simons, R. H.; Callow, J. A.; Lopez, G. A. *Appl. Environ. Microbiol.* **2004**, *70*, 4151–4157.

(22) Statz, A.; Finlay, J.; Dalsin, J.; Callow, M.; Callow, J. A.; Messersmith, P. B. *Biofouling* **2006**, *22*, 391–399.

(23) Callow, M. E.; Jennings, A. R.; Brennan, A. B.; Seegert, C. E.; Gibson, A.; Wilson, L.; Feinberg, A.; Baney, R.; Callow, J. A. *Biofouling* **2002**, *18*, 237–245.

(24) Hoipkemeier-Wilson, L.; Schumacher, J. F.; Carman, M. L.; Gibson, A. L.; Feinberg, A. W.; Callow, M. E.; Finlay, J. A.; Callow, J. A.; Brennan, A. B. *Biofouling* **2004**, *20*, 53–63.

(25) Carman, M. L.; Estes, T. G.; Feinberg, A. W.; Schumacher, J. F.; Wilkerson, W.; Wilson, L. H.; Callow, M. E.; Callow, J. A.; Brennan, A. B. *Biofouling* **2006**, *22*, 11–21.

(26) Bowen, J.; Pettitt, M. E.; Kendall, K.; Leggett, G. J.; Preece, J. A.; Callow, M. E.; Callow, J. A. *J. R. Soc. Interface* **2007**, *4*, 473–477.

(27) Callow, J. A.; Callow, M. E. In *Antifouling Compounds: Vol. 42 Marine Molecular Biotechnology, Progress in Molecular and Subcellular Biology*; Fusetani, N., Clare, A. S., Eds.; Springer-Verlag: Berlin, 2006; pp 141–170.

(28) Thompson, S. E. M.; Callow, J. A.; Callow, M. E.; Wheeler, G. L.; Taylor, A. R.; Brownlee, C. *Plant Cell Environ.* **2007**, *30*, 733–744.

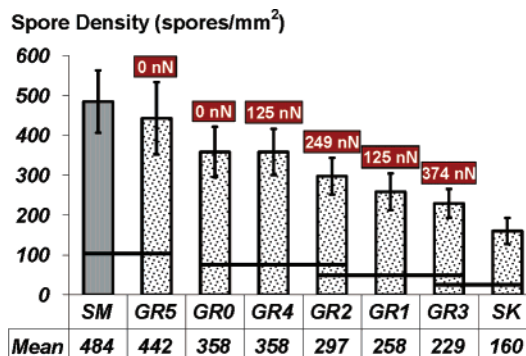


**Figure 5.** Mean spore (*Ulva*) density ( $\pm$ standard error,  $n = 3$ , counts = 30 per  $n$ ) measured and calculated for each PDMS<sub>e</sub> surface studied ( $3 \mu\text{m}$  feature height for all engineered topographies). The experimental design included a positive (smooth, i.e., no topography, PDMS<sub>e</sub> surface, SM) and negative (Sharklet AF PDMS<sub>e</sub> surface, SK) standard. Gradient surfaces included 0 nN force gradient (GR5 and GR0), 125 nN force gradient (GR1 and GR4), 249 nN force gradient (GR2), and 374 nN force gradient (GR3). Horizontal bars indicated significantly different groups (SNK test,  $p < 0.05$ ).

**Table 1.** Sessile Drop Water Contact Angle for PDMS<sub>e</sub> Surfaces

surface type <sup>a</sup>	mean contact angle (deg $\pm$ SD)	surface type <sup>a</sup>	mean contact angle (deg $\pm$ SD)
GR0	138 $\pm$ 3	GR4	135 $\pm$ 2
GR1	134 $\pm$ 3	GR5	137 $\pm$ 4
GR2	136 $\pm$ 1	SK	135 $\pm$ 2
GR3	134 $\pm$ 4	SM	112 $\pm$ 5

<sup>a</sup> GR0–GR5 = gradients surfaces 0–5; SK = Sharklet AF; SM = smooth PDMS<sub>e</sub> surface (no engineered topography modification)

within the lateral plane of the membrane (plasma membrane) of a settling cell or microorganism during initial contact. This apparent stress gradient and nonequilibrium state will function to destabilize and disrupt normal cell function, specifically settlement (attachment). In order to settle and gain stability on the surface, the cell/microorganism will need to provide energy to adjust its contact area on each topographical feature such that the stresses are equal. However, the energy necessary for the cell/microorganism to achieve this equilibrium state may be thermodynamically unfavorable and it will leave and probe another area to settle. When designed at the appropriate dimensions, the stress on a cell membrane is controlled by the bending moment or stiffness of the topographical feature of which it is in contact. The geometric dimensions including width, length, and height of the topographical feature as well as the modulus of the base material define its stiffness. By introducing geometric variations in features contained in the engineered topography, an effective force gradient between neighboring topographical features will be developed. If a cell simultaneously contacts two topographical features of varying geometries, also of inherently different stiffness values, the stress exerted on the membrane from one feature will differ from the stress exerted on the membrane from the other, geometrically dissimilar feature (Figure 1). This difference in forces will cause a gradient within the lateral plane of the cell membrane and a nonequilibrium state that will cause a cell/microorganism to make a choice between providing the energy to create an equilibrium state (i.e., forces balanced) or move to a different area to settle and adhere.

It is postulated that a critical interaction must be achieved between the topographical surface and the settling cell/organism

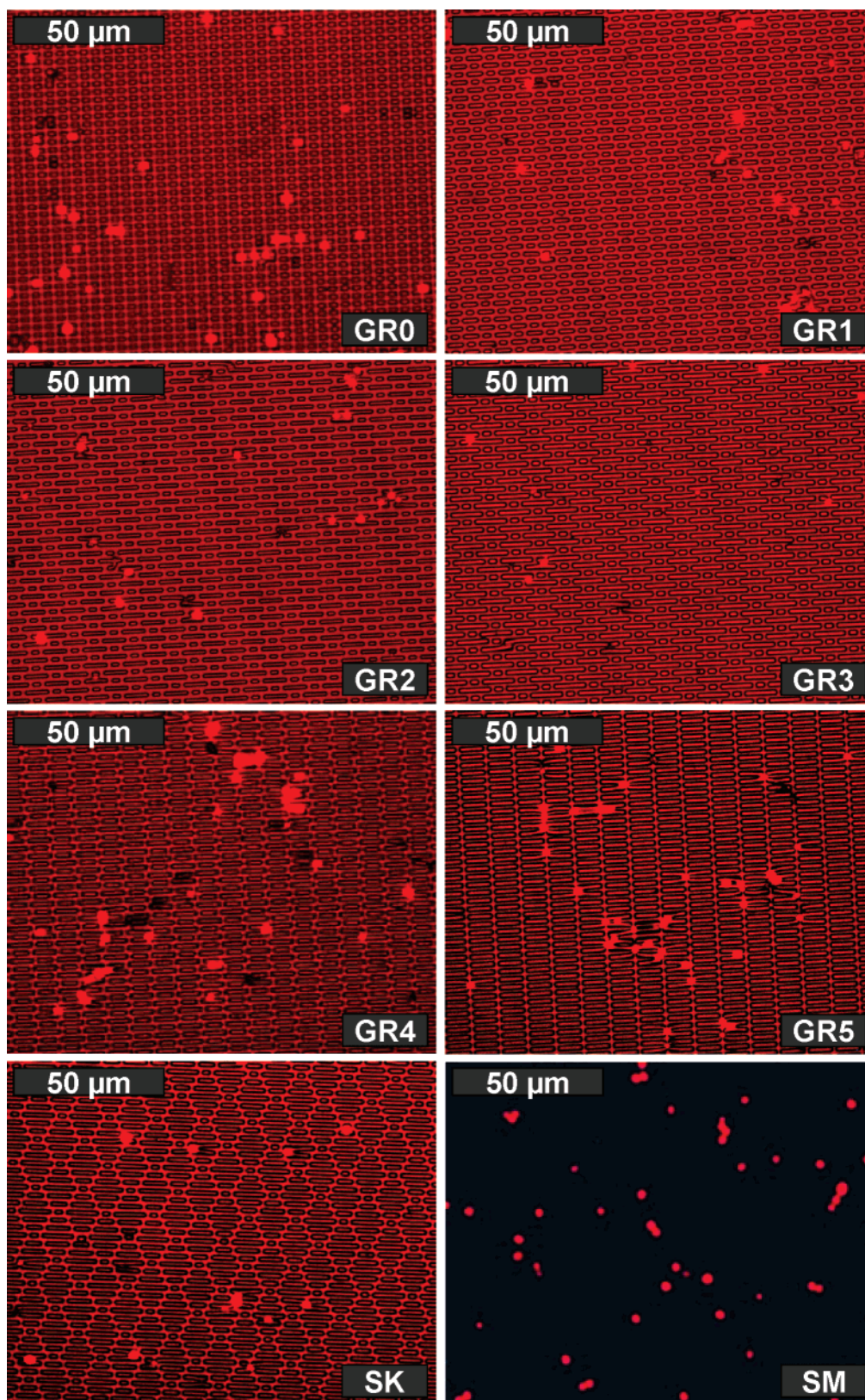


**Figure 6.** Representative light micrographs, obtained by a mixture of epifluorescence and transmitted light, of spores (*Ulva*) settled on PDMS surfaces including gradient surfaces 0–5 (GR0–GR5), Sharklet AF (SK), and uniformly smooth (SM) surface. Spores in these images appear as red spots approximately 5  $\mu\text{m}$  in diameter due to the autofluorescence of chlorophyll.

for the designed nanoforce gradients to be sensed by a cell/organism. The following are hypothesized key elements of the interactions:

(1) The cell/organism must remain on the topographical features and not be able to settle between features. The latter will occur if the protruding topographical features are spaced apart at a

greater distance than the width of the cell/organism. This will allow the cell/organism to fit in-between protruding features and settle/attach to an apparent flat surface.

(2) The cell/organism must not be able to contact and settle its entire cell mass on one single feature. If the width of the top of a protruding topographical feature greatly exceeds (i.e., greater

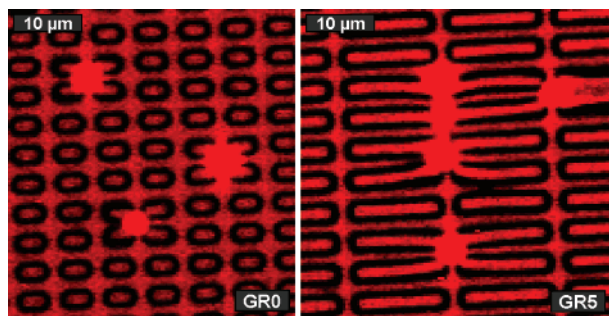


**Figure 7.** Magnified light micrographs showing the preferred settlement location of spores relative to the topographical features on GR0 and GR5.

than 4 times) the width of the cell/organism, settlement/attachment can occur entirely on one individual topographical feature. The force gradient design requires simultaneous contact between two features.

(3) If a cell/organism is bridged between two topographical features, the cell/organism must not be able to contact the floor between features. This will occur if the topographical aspect ratio (feature height/feature width) becomes small (i.e., less than 1) so that it no longer has a physical influence on the cell/organism. When the aspect ratio is small enough such that the cell/organism can contact the recessed floor between protruding features, the maximum amount of surface area contact, even higher than a flat surface, will occur.

A set of feature dimensions (feature width = 2  $\mu\text{m}$ , spacing = 2  $\mu\text{m}$ , and height = 3  $\mu\text{m}$ ) that have shown antifouling efficacy against spores of *Ulva* has been determined.<sup>16</sup> With these critical feature dimensions fixed, the length of each engineered topographical feature was varied from 4 to 16  $\mu\text{m}$  (Figure 2). Micrometer-sized posts of a polydimethylsiloxane elastomer (PDMS<sub>e</sub>) have previously been modeled as linearly elastic cantilever beams under pure bending.<sup>29</sup> Applying this model, the amount of lateral force required to cause an end deflection of 10% for each topographical feature was estimated (Figure 2) using eq 1

$$F = \left( \frac{3EI}{L^3} \right) y \quad (1)$$

where  $F$  is the applied force,  $E$  is the modulus of elasticity,  $I$  is the rectangular moment of area,  $L$  is the height of the feature, and  $y$  is the end deflection distance.<sup>30</sup> The modulus of elasticity for the particular PDMS<sub>e</sub> system used in this study is approximately 1.4 MPa.<sup>31</sup> Deflection forces ranged from 125 nN for the 4  $\mu\text{m}$  length element up to 498 nN for the 16  $\mu\text{m}$  length element (Figure 2). Force gradients were created by combining the various modeled elements into a two-element engineered topography at a fixed feature spacing of 2  $\mu\text{m}$  (Figure 3).

### III. Experimental Design

**Design of *Ulva*-Specific Nanoforce Gradients.** Modeled topographical features (Figure 2) were combined into two-element engineered topographies at the critical feature spacing of 2  $\mu\text{m}$  for

the spores of *Ulva* (Figure 3). Force gradients were characterized as the difference between the modeled deflection forces for each topographical feature. Gradient surface 1 (GR1) was designed with the 4  $\mu\text{m}$  length feature neighbored by the 8  $\mu\text{m}$  length feature and an estimated nanoforce gradient of 125 nN. Gradient surface 2 (GR2) contained the 4 and 12  $\mu\text{m}$  length features (gradient = 249 nN), gradient surface 3 (GR3) included the 4 and 16  $\mu\text{m}$  length features (gradient = 374 nN), and gradient surface 4 (GR4) was designed with the 8 and 12  $\mu\text{m}$  features (gradient = 125 nN). Gradient surface 0 (GR0), 4  $\mu\text{m}$  length feature, and gradient surface 5 (GR5), 12  $\mu\text{m}$  length feature, were designed to contain no force gradient as neighboring features were identical. For these engineered topographies fabricated in PDMS<sub>e</sub>, it was hypothesized that spore settlement would decrease with an increase in the force gradient. A smooth PDMS<sub>e</sub> surface (SM) was included in the experiment as a positive standard and the most effective engineered topography to date for reducing spore settlement,<sup>16</sup> Sharklet AF (SK), was included as an experimental negative standard.

**Materials.** A platinum-catalyzed PDMS<sub>e</sub>, SILASTIC T-2 (Dow Corning), was used as the base material for engineered topographical modification. The elastomer was prepared by mixing ten parts resin and one part curing agent by weight for 5 min. The mixture was degassed under vacuum (28–30 in. Hg) for 30 min, removed, and allowed to cure for 24 h at  $\sim 22$  °C against negative topographical molds.

**Engineered Topography Mold Fabrication.** Negative molds of the engineered topographies based on the force gradient pattern designs (Figure 3) were fabricated in silicon wafers. The gradient pattern designs were transferred to photoresist-coated silicon wafers using previously described photolithographic techniques.<sup>31</sup> Patterned silicon wafers were deep reactive ion etched to a depth of 3  $\mu\text{m}$  for all pattern designs. Wafers were then cleaned (i.e., stripped of photoresist) with an O<sub>2</sub> plasma etch. Hexamethyldisilazane was vapor deposited on the processed silicon wafers to methylate the surfaces in order to prevent adhesion to PDMS<sub>e</sub> during the replication process.

**Engineered Topography Replication.** Engineered topographies were transferred to PDMS<sub>e</sub> from replication of the patterned and etched silicon wafers. The resultant engineered topographies contained features projecting from the surface at heights respective of the etch depth. Pattern fidelity was evaluated using light and scanning electron microscopy (Figure 4).

**Contact Angle Characterization.** The three-phase water contact angle for each PDMS<sub>e</sub> surface was measured using a Ramé-Hart contact angle goniometer with an automated drop dispenser and video capture system. The reported contact angle ( $\pm$ standard deviation) represents the average contact angle for seven to nine 5  $\mu\text{L}$  drops of nanopure water with resistivity greater than 17 M $\Omega$  cm.

**Sample Preparation for *Ulva* Settlement Assay.** The *Ulva* zoospore settlement assay was conducted with 76 mm  $\times$  25 mm glass microscope slides coated with smooth and engineered topographical PDMS<sub>e</sub> surfaces. Glass slides containing engineered topography in PDMS<sub>e</sub> were fabricated using a two-step curing process as previously described.<sup>25</sup> The resultant slide (ca. 1 mm thickness) contained an adhered PDMS<sub>e</sub> film with a 25 mm  $\times$  25 mm area containing topography bordered on both sides by 25 mm  $\times$  25 mm smooth areas.

***Ulva* Zoospore Settlement Assay.** Three replicates of each PDMS<sub>e</sub> surface, permanently adhered to glass microscope slides, were evaluated for settlement of spores of *Ulva*. Engineered topographies included gradient surfaces, GR0–GR5 (Figure 4), at a feature height of 3  $\mu\text{m}$ . A uniformly smooth PDMS<sub>e</sub> sample (SM, Figure 4) was included as a positive standard. The Sharklet AF (SK, Figure 4) surface at a feature height of 3  $\mu\text{m}$  was included as a negative standard.

Fertile plants of *U. linza* were collected from Wembury Beach, UK (50°18'N, 4°02'W), and the zoospores were released and prepared for settlement experiments as previously described.<sup>23</sup> Surfaces were presoaked in nanopure water for 4 days prior to the assay in order for the surfaces to fully wet. Samples were transferred to artificial seawater (ASW; Tropic Marin) for 1 h prior to experimentation without exposure to air. Samples were then rapidly transferred to

(29) Tan, J. L.; Tien, J.; Pirone, D. M.; Gray, D. S.; Bhadriraju, K.; Chen, C. *Proc. Natl. Acad. Sci. U.S.A.* **2003**, *100*, 1484–1489.

(30) Matthews, C. *ASME Engineer's Data Book*, 2nd ed.; ASME Press: New York, 2005; Chapter 6.

(31) Feinberg, A. W.; Gibson, A. L.; Wilkerson, W. R.; Seeger, C. A.; Wilson, L. H.; Zhao, L. C.; Baney, R. H.; Callow, J. A.; Callow, M. E.; Brennan, A. B. In *Synthesis and Properties of Silicones and Silicone-Modified Materials*; Clarson, S. J., Fitzgerald, J. J., Owen, M. J., Smith, S. D., Van Dyke, M. E., Eds.; ACS Symposium Series 838; American Chemical Society: Washington DC, 2003; pp 196–211.

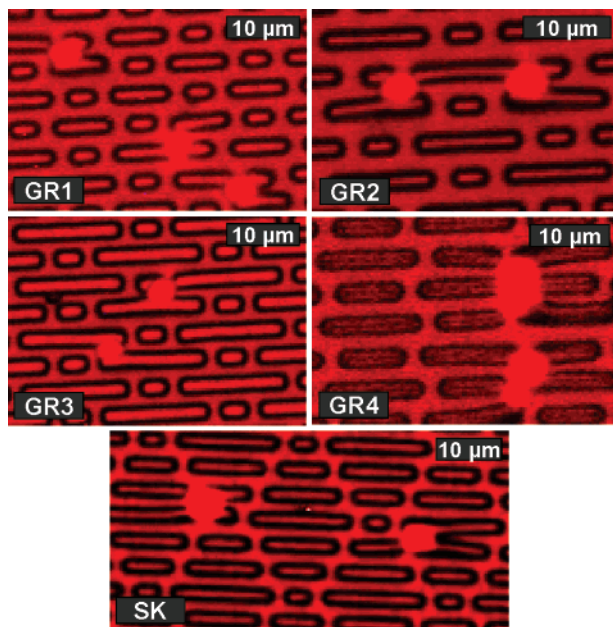


**Figure 8.** Magnified light micrographs showing the preferred settlement location of spores relative to the topographical features on GR1–GR4 and SK.

assay dishes. Ten milliliters of spore suspension (adjusted to  $2 \times 10^6 \text{ mL}^{-1}$ ) was added to each dish and placed in darkness for 60 min. The slides were rinsed to wash away unsettled (swimming) zoospores and fixed with 2% glutaraldehyde in ASW as previously described.<sup>23</sup>

Settled spores were quantified using a Zeiss epifluorescence microscope connected to a Zeiss Kontron 3000 image analysis system. Thirty counts were obtained from each of three replicates at 1 mm intervals along both the vertical (15) and horizontal (15) axes of the slide.

**Statistical Methods.** Spore density was reported as the mean number of settled spores per  $\text{mm}^2$  from 30 counts on each of three replicate slides per surface type  $\pm$  standard error ( $n = 3$ ). Statistical differences between surfaces were evaluated using a nested analysis of variance (ANOVA) followed by the Student–Newman–Keuls (SNK) test for multiple comparisons.<sup>32</sup> Replicate slides (three) were treated as nested variables within each surface type. Each replicate was associated with 30 random spore density counts. Statistical computations were completed using Minitab 14 statistical software package.

#### IV. Results

Static surface energy measurements were obtained on each PDMS surface prior to exposure to the zoospores of *Ulva*. The sessile drop water contact angle measured for each engineered topography, including gradient surfaces 1–5 (GR0–GR5) and Sharklet AF (SK), all fell within the range from  $134^\circ \pm 4^\circ$  to  $138^\circ \pm 3^\circ$  (Table 1). The smooth PDMS surface (no engineered topography modification) had a contact angle of  $112^\circ \pm 5^\circ$ .

The mean spore (*Ulva*) density ( $\pm$  standard error,  $n = 3$ , counts = 30 per  $n$ ) was determined for each PDMS surface tested (Figure 5). Significantly different groups are represented by horizontal connecting bars (Figure 5, SNK test  $p < 0.05$ ). The highest spore density ( $484 \pm 78 \text{ spores/mm}^2$ ) was measured on the smooth (SM) positive standard. The negative standard, Sharklet AF, had the lowest measured spore density ( $160 \pm 33 \text{ spores/mm}^2$ ). Surfaces designed to contain no force gradient (0 nN, GR5 and GR0) had the highest ( $442 \pm 91$  and  $358 \pm 63 \text{ spores/mm}^2$ , respectively) spore density values among the gradient

designs. The lowest spore density among gradient surfaces ( $229 \pm 36 \text{ spores/mm}^2$ , 53% reduction relative to smooth) was measured on the surface with the highest modeled force gradient (GR3, 374 nN). The remaining gradient surfaces (GR4,  $358 \pm 58 \text{ spores/mm}^2$ ; GR2,  $297 \pm 46 \text{ spores/mm}^2$ ; and GR1,  $258 \pm 46 \text{ spores/mm}^2$ ) with designed force gradients ranging from 125 to 249 nN all significantly reduced spore density (26, 39, and 47%, respectively) relative to the smooth PDMS surface.

The density and distribution of settled spores relative to topographical features can be seen by inspection of light micrographs obtained by a mixture of epifluorescence and transmitted light (see representative images in Figure 6). Spores appear as red spots, approximately  $5 \mu\text{m}$  in diameter, due to the autofluorescence of chlorophyll. For gradient surfaces containing no force gradient (GR0 and GR5), spores appeared to preferentially settle at the end of the long axis of each feature ( $4 \mu\text{m}$  for GR0,  $12 \mu\text{m}$  for GR5) contacting the short sides ( $2 \mu\text{m}$  in length) of neighboring features (Figure 7). Furthermore, it was observed that spores generally made four points of contact in this area, as opposed to two points of contact when settled between the long sides of each neighboring feature. The preferential settlement location of spores on gradient surface 4 (GR4, Figure 8) was similar (i.e., four points of contact) to that of gradient surface 5 (GR5, Figure 7). Due to the design of gradient surfaces 1–3 (GR1–GR3) and Sharklet AF (SK), spores are only able to make a maximum of three points of contact among the available settlement locations. Spores were observed to be settled in the areas where three points of contact are possible (GR1–GR3 and SK, Figure 8).

#### V. Discussion

The gradient surfaces designed with nanoforce gradients between 125 and 374 nN all significantly reduced the settlement of the zoospores of *Ulva* relative to the smooth PDMS surface. The highest reduction among gradient surfaces, 53%, was for the surface with the highest modeled force gradient (GR3, 374 nN). The gradient surfaces containing no force gradients had the lowest (GR5, 0 nN) and tied for the second lowest (GR0, 0 nN) reduction relative to smooth. The other gradient surfaces with modeled force gradients between 125 and 249 nN all fell within these two limits in terms of reduction relative to the smooth PDMS surface. These results indicated that a force gradient approach, considering the mechanotransduction response of a settling organism/cell, may be an effective conceptual methodology for the design of nonfouling engineered topographies. By designing surface topography that considers the local micrometer-scale effects on the cell membrane rather than the overall surface property of the material (e.g., superhydrophobicity and surface energy), more effective nontoxic antifouling surfaces and models can be developed. In relation to surface properties, the engineered topographies studied, including gradient surfaces and the Sharklet AF, all had static contact angles within the range of  $134^\circ$ – $138^\circ$ , yet yielded significant differences in spore settlement behavior.

The Sharklet AF surface was not designed on the basis of force gradients.<sup>16,25</sup> The design was inspired by nature and modeled after the skin of a shark. However, the Sharklet AF does contain a variety of discrete nanoforce gradients across the surface. By applying the same model to estimate a force gradient between features as with the gradient designs, the same nanoforce gradient (125 nN) was found in three different areas of the topography. These areas occurred between the 4 and  $8 \mu\text{m}$  length features, the 8 and  $12 \mu\text{m}$  length features, and the 12 and  $16 \mu\text{m}$  length features. Although the modeled force gradient was not the highest of the gradient designs, the Sharklet AF surface had the lowest measured spore density of any of the gradient surfaces.

(32) Paulson, D. S. *Applied Statistical Designs for the Researcher*; Marcel Dekker: New York, 2003; Chapter 10.

This, however, could be due to the fact that the Sharklet AF was a more complex four-element engineered topography, compared to the two-element gradient surfaces, and presented a more tortuous surface for the zoospore as it explored the surface. We have already shown that the larger length scale of the Sharklet AF (features  $20\ \mu\text{m}$  wide,  $20\ \mu\text{m}$  spacing,  $40\ \mu\text{m}$  high and lengths scaled by a factor 10) pattern inhibits effectively the settlement of the *Balanus amphitrite* larvae, which is a multicellular organism.<sup>33</sup> In addition, many other engineered topographies, not designed on the basis of force gradients, tested against the Sharklet AF have not been able to match this surface's antifouling effectiveness against the spores of *Ulva*.<sup>16</sup> There still is much to be studied and understood in terms of the unique properties of the Sharklet AF surface that make it such an effective antifouling surface.

## VI. Conclusions

The concept of designed nanoforce gradients using engineered topography presents a new approach for the design of nontoxic,

---

(33) Schumacher, J. F.; Aldred, N.; Callow, M. E.; Finlay, J. A.; Callow, J. A.; Clare, A. S.; Brennan, A. B. *Biofouling* **2007**, *23*, 307–317.

antifouling surfaces. The surface designs rely strictly on a physical perturbation of the membrane or body of the settling cell/organism without the necessity to chemically modify the surface or leach any substances (e.g., biocides) from the base material. This methodology considers the local mechanical effects on the micrometer-scale that engineered topography may impart on a settling organism. This is a unique design approach compared to current theories that only consider optimizing and/or increasing a single, global surface property, such as superhydrophobicity or surface energy. Experimental data for the settlement behavior of the zoospore of *Ulva* on gradient surfaces confirm that the designed nanoforce gradients may be an effective prediction tool for the design of unique nontoxic, antifouling marine and biomedical surfaces.

**Acknowledgment.** A.B.B., J.A.C., and M.E.C. gratefully acknowledge the financial support of the Office of Naval Research (Contract #N00014-02-1-0325 to A.B.B., and Contract #N00014-02-1-0521 to J.A.C. and M.E.C.).

LA703421V